$O(\alpha^2 \ln(\alpha^{-1}))$ corrections in positronium: Hyperfine splitting and decay rate

William E. Caswell
Department of Physics, Brown University, Providence, Rhode Island 02912

G. Peter Lepage
Stanford Linear Accelerator Center, Stanford University, Stanford, California 94305
*and Laboratory of Nuclear Studies, Cornell University, Ithaca, New York 14853**

(Received 7 December 1978)

The authors have analyzed the terms of relative order $\alpha^2 \ln(\alpha^{-1})$ that come from annihilation kernels in positronium, and have found a contribution of $\alpha^6 \ln(\alpha^{-1}) m_e/24$ to positronium hyperfine splitting from annihilation kernels, including several new contributions. The resulting hyperfine splitting is 203.4003 GHz, with terms of order $\alpha^6 m_e/2 \sim 0.01$ GHz uncomputed. The contributions to the decay rates of ortho- and parapositronium have also been calculated. For orthopositronium the result is $-\alpha^2 \ln(\alpha^{-1})\Gamma_0/3$. The authors present in more detail the theoretical analysis leading to their previous $\alpha\Gamma_0$ calculation and improve on the numerical results. The resulting theoretical orthopositronium decay rate is 7.0386 ± 0.0002 μsec^{-1}, with terms of order $\alpha^2\Gamma_0 = 0.0004$ μsec^{-1} uncalculated.

I. INTRODUCTION

The study of bound states in quantum electrodynamics (QED) is important as a precise test of QED as the theory of electromagnetic interactions. It is also a laboratory for developing techniques for calculating bound-state parameters in other relativistic field theories. Recently, alternatives to the Bethe-Salpeter (BS) equation for two-body bound states have been introduced. They have been successfully applied to the organization and calculation of order $\alpha^2 \ln(\alpha^{-1}) E_F$ contributions to hyperfine splitting (hfs, the difference between spin-1 and spin-0 ground-state energies) in positronium $(e^- e^+)$ and muonium $(e^- \mu^+)$.[1] Positronium, with equal-mass constituents, particularly tests two-body, relativistic equations. A simple, exact, Schrödinger-like formalism has been used to calculate the contributions from infinite Coulomb-exchange graphs to $O(\alpha^2 E_F)$.[2]

In this paper we calculate the $O[\alpha^6 \ln(\alpha^{-1}) m_e]$ contributions to the hfs of positronium (Ps) coming from annihilation kernels. These terms are quite important to the comparison of theory with experiment as $\alpha^6 \ln(\alpha^{-1}) m_e \sim 92$ MHz and the experimental uncertainty is only 1.2 MHz. Picking out the logarithmic terms in annihilation graphs is quite simple using the exact Schrödinger-like formalism of II,[2] and here we present the first complete calculation of all such terms. Some of these terms were discovered by Owen[3] and by Barbieri and Remiddi.[3,4] Important new logarithmic terms are found, and in Table I we compare the new theoretical value to recent precision experimental results.[5,6] The correct theoretical value was quoted in I.[1] The uncomputed terms of $O(\alpha^6 m_e/2)$ are an order of magnitude larger than the experimental uncertainties, and can easily be large enough to bring theory into agreement with experiment.

We first became interested in the logarithmic terms in order to make more precise the theoretical prediction of the decay rate of orthopositronium (o-Ps: $n=1, J=S=1$). We call the lowest-order decay rate of o-Ps Γ_0.[7] The calculation of the $O(\alpha\Gamma_0)$ decay rate[8] had left a large discrepancy between the theoretical prediction and the best precision measurements of the decay rate.[9] The calculation of Sec. II is trivially modified to give the terms of $O[\alpha^2 \ln(\alpha^{-1})\Gamma_0]$. The resulting coefficient, which we calculate in Sec. III, is quite small. More recent experiments have significantly decreased the discrepancy between theory and experiment. The theoretical and experimental values are compared in Table II (the new theoretical value was quoted in Ref. 11). There remain uncalculated terms of $O(\alpha^2\Gamma_0) \sim 0.0004$ μsec^{-1}. If these have a small coefficient (less than 5) there is still a small but significant disagreement with the most recent

TABLE I. Comparison of theory and experiment for positronium hfs. Terms of $O(\alpha^6 m_e/2) \sim 0.01$ GHz are not yet computed.

Theory	
$O(\alpha^4 m_e, \alpha^5 m_e)$	203.381 GHz
$\frac{5}{24}\alpha^6 m_e \ln\alpha^{-1}$	0.019 GHz
Total theory	203.400 GHz
Experiment	
Ref. 5	203.3849 (12) GHz
Ref. 6	203.3870 (16) GHz

TABLE II. Comparison of theory and experiment for orthopositronium decay rate. Terms of order $\alpha^2\Gamma_0 \sim 0.0004\ \mu\text{sec}^{-1}$ have not yet been computed.

Theory			
Ref. 8	Γ_0	7.211 2	μsec^{-1}
Ref. 7 and Appendix	$(-10.266 \pm 0.011)\frac{\alpha}{\pi}\Gamma_0$	$-0.172\,0 \pm 0.000\,2$	μsec^{-1}
Sec. III	$-\frac{1}{3}\alpha^2 \ln(\alpha^{-1})\Gamma_0$	$-0.000\,63$	μsec^{-1}
Total theory		$7.038\,6 \pm 0.000\,16$	μsec^{-1}
Experiment			
Ref. 10	gas	7.058 ± 0.015	μsec^{-1}
Ref. 11	gas	7.056 ± 0.007	μsec^{-1}
Ref. 12	vacuum	7.050 ± 0.013	μsec^{-1}

measurements of o-Ps decay in gas.[10,11] However, a new vacuum measurement[12] agrees with the theoretical value, though its quoted systematic error is larger than that of the gas measurements.

In the Appendix we review the calculation of the $O(\alpha\Gamma_0)$ contribution to the decay rate of o-Ps. We write down the explicit perturbation series and show how to reduce the problem to one where the electron and positron may be placed on-shell. An improved numerical integration result leaves us with a statistical error which is negligible compared to the uncalculated $O(\alpha^2\Gamma_0)$ contributions to the decay rate. The $O(\alpha)$ rate of Table II includes this improved result.

II. CALCULATION OF THE $\alpha^2 \ln(\alpha^{-1})E_A$ CONTRIBUTIONS TO HYPERFINE SPLITTING

In this section we will calculate the $\alpha^2 \ln(\alpha^{-1})E_A$ contributions to Ps hfs arising from annihilation kernels. We will use the formalism of II. E_A is the lowest-order annihilation contribution to hfs (Fig. 1). Equations (2.12) and (3.5c) of II imply

$$E_A = \langle i\tilde{K}_A \rangle \simeq |\phi(0)|^2 (e^2/2m^2) \simeq \tfrac{1}{4}\alpha^4 m . \qquad (2.1)$$

Here $m(=2m_R)$ is the mass of the bound particle. The exact perturbation series for the energy to second order is recorded in Fig. 4(a) of II [see also Eq. (2.12) of II]. The terms which are relevant to $O[\alpha^2 \ln(\alpha^{-1})]$ are displayed in Fig. 2. Single-photon annihilation does not affect parapositronium ($n=1$, $J=S=0$), by charge conjugation invariance,

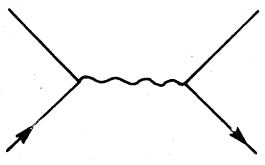

FIG. 1. Lowest-order annihilation kernel.

so we simply compute the energy of o-Ps coming from single-photon annihilation kernels.

We are interested in calculating terms which have logarithms of the coupling. The three-momenta which are important for these terms are those sensitive to both the binding and the electron mass. We, therefore, can approximate $\gamma \ll |\vec{p}| \ll m$, where $\gamma = \alpha m_R = \alpha m/2$. We will call this region the logarithmic region, and the region $p \sim \gamma$ the nonrelativistic region (NR). Physically, the lower momentum limit comes from the binding and the finite size of the atom [$p \sim$ (Bohr radius)$^{-1} \sim \gamma$]. The upper limit comes from the relativistic falloff

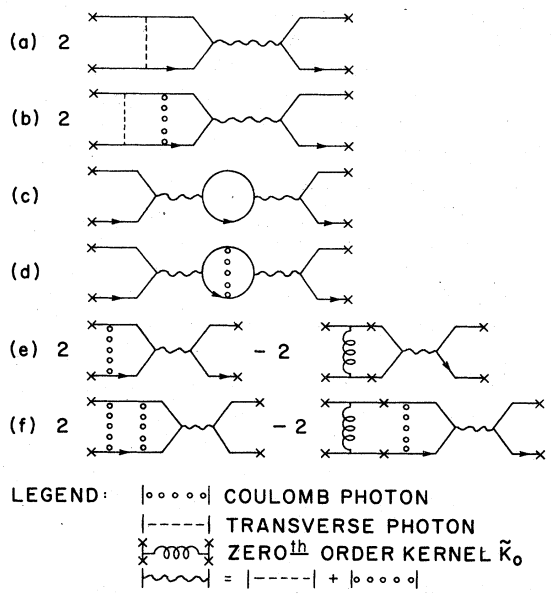

FIG. 2. Kernels contributing to $\alpha^2 \ln(\alpha^{-1})E_A$ in positronium. The pairs of x's mean that the corresponding lines are projected onto on-shell spinors [Eq. (2.4)], and the relative energy is set to zero.

of the electron propagator $1/(\not{p}-m)$ $(p \sim m)$.

The bound particles (electron and positron, or 1 and 2), being loosely bound, are to a good approximation near their mass shells. In the logarithmic region all internal fermions are also near mass shell since each momentum transfer is much less than the mass. Neglecting retardation in the interaction kernels (see below), we can then replace internal fermion propagators by nonrelativistic propagators. For a ladder graph (Fig. 3) we obtain[13]:

$$i\int \frac{d^4k}{(2\pi)^4} K_1(\vec{p},\vec{k},P)\, \frac{i}{(\tau_1 P + \not{k} - m)} \frac{i}{(\tau_2 P - \not{k} - m)} K_2(\vec{k},\vec{q},P)$$
$$\simeq \int \frac{d^3k}{(2\pi)^3}\, i K_1(\vec{p},\vec{k},P)\, \frac{\Lambda_+^{(1)}(\vec{k})\Lambda_+^{(2)}(\vec{k})}{P-2E(k)}\, iK_2(\vec{k},\vec{q},P), \tag{2.2}$$

where

$$\Lambda_+(\vec{k}) = \frac{E(k)\gamma^0 - (\vec{k}\cdot\gamma - m)}{2E(k)} = \frac{\sum_s u(\vec{k},s)\,\bar{u}(\vec{k},s)}{2E(k)}$$

and $E(k) = (\vec{k}^2 + m^2)^{1/2}$. Note that in the logarithmic region

$$P^0 - 2E(k) \approx \epsilon - (\vec{k}^2/m) = -(\vec{k}^2+\gamma^2)/m\,. \tag{2.3}$$

Thus all interactions of interest for the logarithmic terms can be written in the on-shell (tilde) formalism of II[14] using the definition [(2.9) of II]:

$$\tilde{K}(\vec{k},\vec{q},P)_{\lambda'\mu',\lambda\mu} = \frac{\bar{u}^{(1)}(\vec{k},\lambda')\,\bar{u}^{(2)}(-\vec{k},\mu')}{[4E_1(\vec{k})E_2(\vec{k})]^{1/2}} \times \bar{K}(\vec{k},\vec{q},P) \times \frac{u^{(1)}(\vec{q},\lambda)\,u^{(2)}(-\vec{q},\mu)}{[4E_1(\vec{q})E_2(\vec{q})]^{1/2}}\,. \tag{2.4}$$

Then any loop integration (by Eq. 2.2) has the simple form

$$\int \frac{d^3k}{(2\pi)^3}\, i\tilde{K}_1(\vec{p},\vec{k},P)\, \frac{-m}{(\vec{k}^2+\gamma^2)}\, i\tilde{K}_2(\vec{k},\vec{q},P). \tag{2.5}$$

The kernels which appear in Fig. 2 are the following (in the tilde formalism, see II):

(a) Difference kernel [Figs. 2(e), 2(f)]:

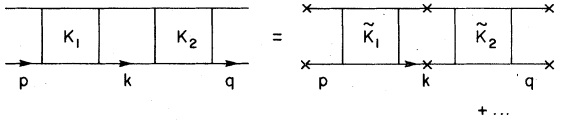

FIG. 3. Breakup of a ladder diagram into two kernels that are then projected on-shell.

$$i\delta\tilde{K}_C = i(\tilde{K}_C - \tilde{K}_0) = \frac{-e^2}{|\vec{k}-\vec{q}|^2} \times \left(\frac{\vec{k}\cdot\vec{q}}{m^2} - \frac{\vec{k}^2+\vec{q}^2+4\vec{k}\cdot\vec{q}}{8m^2} - \frac{\epsilon}{4m} + \frac{i\vec{k}\times\vec{q}\cdot\vec{\sigma}_1}{4m^2} + \frac{i\vec{k}\times\vec{q}\cdot\vec{\sigma}_2}{4m^2}\right). \tag{2.6a}$$

(b) Single-transverse-photon exchange [Figs. 2(a), 2(b)]:

$$i\tilde{K}_T = \frac{e^2}{|\vec{k}-\vec{q}|^2}\left(\frac{(\vec{k}\cdot\vec{q})^2 - \vec{k}^2\vec{q}^2}{m^2|\vec{k}-\vec{q}|^2} - \frac{i\vec{k}\times\vec{q}\cdot(\vec{\sigma}_1+\vec{\sigma}_2)}{2m^2} + \frac{(\vec{k}-\vec{q})\times\vec{\sigma}_1\cdot(\vec{k}-\vec{q})\times\vec{\sigma}_2}{4m^2}\right). \tag{2.6b}$$

(c) Single-photon annihilation:

$$i\tilde{K}_A = (e^2/8m^2)(3+\vec{\sigma}_1\cdot\vec{\sigma}_2)\,. \tag{2.6c}$$

(d) Single Coulomb exchange:

$$i\tilde{K}_C = -e^2/|\vec{k}-\vec{q}|^2\,. \tag{2.6d}$$

The $\alpha^2\ln(\alpha^{-1})$ terms arising from annihilation kernels all come from overlapping electron loop integrals. All propagators (where we have picked out the particle one pole) are quadratic in the three-momentum in the logarithmic region. It is thus impossible to obtain a logarithmically divergent integral of the form $\int d^3p/p^3$ from a single loop. We need two loops and a logarithmic divergence of the form $\int d^3p\, d^3q/p^2|\vec{p}-\vec{q}|^2q^2$. The logarithmic contributions of these integrals are listed in Table III, taken from I. The requirement that the resulting integral have overlapping electron loop integrals means that Figs. 1 and 2(c) will not contribute logarithmic terms to the energy.

We now proceed to calculate the $\alpha^2\ln(\alpha^{-1})E_A$ contributions to hfs. We will in all cases take the ratio to the lowest-order annihilation contribution E_A [Eq. (2.1)]. The right-hand wave function will always be integrated out, and the left-hand wave

TABLE III. Table of integrals required for analytic evaluations.

$$\int_{\sim\alpha m}^{\sim m} \frac{d^3k}{k^4}\frac{d^3q}{q^4}\frac{f(k,q)}{|\vec{k}-\vec{q}|^2} = K\pi^4\ln\alpha^{-1}$$

$f(k,q)$	K
k^4, q^4	0
k^2q^2	4
$k^2k\cdot q, q^2k\cdot q$	2
$(k\cdot q)^2$	2

function will be removed when it does not contribute to logarithmic terms [2(b), 2(d), 2(f)]. The diagrams will be labeled by the kernels they contain [Eq. (2.6)]. The kernels will in all cases be strung together using Eq. (2.5).

The contribution from one transverse photon [Fig. 2(a)] is

$$\begin{aligned}\delta E_T &= 2\frac{\gamma^3}{\pi}\int \frac{\gamma}{\pi^2}\frac{d^3p}{(\vec{p}^2+\gamma^2)^2} i\tilde{K}_T(\vec{p},\vec{q})\frac{d^3q}{(2\pi)^3} \\ &\quad\times \frac{1}{P_0 - E_1(q) - E_2(q)} i\tilde{K}_A(\vec{q},\vec{r})\frac{\gamma}{\pi^2} \\ &\quad\times \frac{d^3r}{(\vec{r}^2+\gamma^2)^2} \\ &= 2E_A \int \frac{\gamma}{\pi^2}\frac{d^3p}{(\vec{p}^2+\gamma^2)^2} i\tilde{K}_T(\vec{p},\vec{q}) \\ &\quad\times \frac{-m}{(\vec{q}^2+\gamma^2)}\frac{d^3q}{(2\pi)^3} \\ &= -\frac{m^2\alpha}{8\pi^5}E_A \int \frac{d^3p}{(\vec{p}^2+\gamma^2)^2}\frac{e^2}{|\vec{p}-\vec{q}|^2} \\ &\quad\times \frac{(\vec{p}\cdot\vec{q})^2 - \vec{p}^2\vec{q}^2}{m^2|\vec{p}-\vec{q}|^2}\frac{d^3q}{(\vec{q}^2+\gamma^2)} \\ &= \alpha^2\ln(\alpha^{-1})E_A . \end{aligned} \tag{2.7}$$

In the second line we have removed the lowest-order contribution, E_A. We used Table III (letting $q \to -p+q$) to get the last line. The second term of $i\tilde{K}_T$ [Eq. (2.6b)] vanishes by spherical symmetry of the wave function, and the last term has no $\ln(\alpha^{-1})$ contribution after we average over the spin $(\sigma_1^i\sigma_2^j \to \delta^{ij}\frac{1}{3}\langle\vec{\sigma}_1\cdot\vec{\sigma}_2\rangle = \frac{1}{3}\delta^{ij}$ in o-Ps) since that part of the kernel is a δ-function (there is then no denominator term coupling the two electron loop integrals).

The transverse followed by a Coulomb, Fig. 2(b) (we have here removed both wave functions):

$$\begin{aligned}\delta E_{TC} &= 2\frac{\gamma^3}{\pi}\int i\tilde{K}_T(0,\vec{p})\frac{-m}{\vec{p}^2+\gamma^2}\frac{d^3p}{(2\pi)^3} i\tilde{K}_C(\vec{p},\vec{q}) \\ &\quad\times \frac{-m}{\vec{q}^2+\gamma^2}\frac{d^3q}{(2\pi)^3} i\tilde{K}_A(\vec{q},0) \\ &= 2E_A\frac{m^2}{(2\pi)^6}\int \frac{e^2}{|\vec{p}|^2}\frac{(\vec{p}\times\vec{\sigma}_1)\cdot(\vec{p}\times\vec{\sigma}_2)}{4m^2} \\ &\quad\times \frac{d^3p}{(\vec{p}^2+\gamma^2)}\frac{-e^2}{|\vec{p}-\vec{q}|^2}\frac{d^3q}{(\vec{q}^2+\gamma^2)} \\ &= -\tfrac{1}{3}\alpha^2\ln(\alpha^{-1})E_A . \end{aligned} \tag{2.8}$$

In the third line we kept only the last term of $\tilde{K}_T$ as the first two vanish for one momentum zero. We again average over spins before doing the integral. This result agrees with that found by Barbieri and Remiddi.[4]

The annihilation kernel followed by a Coulomb [Fig. 2(d)] contributes.

$$\begin{aligned}\delta E_{AC} &= \frac{\gamma^3}{\pi}\int i\tilde{K}_A(0,\vec{p})\frac{-m}{\vec{p}^2+\gamma^2}\frac{d^3p}{(2\pi)^3} i\tilde{K}_C(\vec{p},\vec{q}) \\ &\quad\times \frac{-m}{\vec{q}^2+\gamma^2}\frac{d^3q}{(2\pi)^3} i\tilde{K}_A(\vec{q},0) \\ &= E_A\frac{e^2}{2}\frac{1}{(2\pi)^6}\int \frac{d^3p}{\vec{p}^2+\gamma^2}\frac{-e^2}{|\vec{p}-\vec{q}|^2}\frac{d^3q}{\vec{q}^2+\gamma^2} \\ &= -\tfrac{1}{2}\alpha^2\ln(\alpha^{-1})E_A . \end{aligned} \tag{2.9}$$

This value agrees with that found by Owen[3] and by Barbieri, Christillin, and Remiddi.[3]

A single Coulomb kernel [Fig. 2(e)], with the iteration of the unperturbed kernel removed (i.e., a difference kernel), contributes

$$\begin{aligned}\delta E_D &= 2\frac{\gamma^3}{\pi}\int \frac{\gamma}{\pi^2}\frac{d^3p}{(\vec{p}^2+\gamma^2)^2} i\delta\tilde{K}_C(\vec{p},\vec{q})\frac{d^3q}{(2\pi)^3} \\ &\quad\times \frac{-m}{\vec{q}^2+\gamma^2} i\tilde{K}_A(\vec{q},0) \\ &= E_A\left(-\frac{\alpha m^2}{8\pi^5}\right)\int \frac{d^3p}{(\vec{p}^2+\gamma^2)^2}\frac{-e^2}{|\vec{p}-\vec{q}|^2}\frac{d^3q}{(\vec{q}^2+\gamma^2)} \\ &\quad\times\left(\frac{\vec{p}\cdot\vec{q}}{m^2} - \frac{\vec{p}^2+\vec{q}^2+4\vec{p}\cdot\vec{q}}{8m^2}\right) \\ &= \tfrac{1}{4}\alpha^2\ln(\alpha^{-1})E_A . \end{aligned} \tag{2.10}$$

The last two terms of $\delta\tilde{K}_C$ vanish by symmetry of the positronium wave function.

Two Coulombs (with a single iteration of the unperturbed kernel removed), Fig. 2(f), contributes

$$\begin{aligned}\delta E_{DC} &= 2\frac{\gamma^3}{\pi}\int i\delta\tilde{K}_C(0,\vec{p})\frac{-m}{\vec{p}^2+\gamma^2}\frac{d^3p}{(2\pi)^3} \\ &\quad\times i\tilde{K}_C(\vec{p},\vec{q})\frac{-m}{\vec{q}^2+\gamma^2}\frac{d^3q}{(2\pi)^3} i\tilde{K}_A(\vec{q},0) \\ &= 2E_A\frac{m^2}{(2\pi)^6}\int \frac{e^2}{8m^2}\frac{d^3p}{\vec{p}^2+\gamma^2}\frac{-e^2}{|\vec{p}-\vec{q}|^2}\frac{d^3q}{\vec{q}^2+\gamma^2} \\ &= -\tfrac{1}{4}\alpha^2\ln(\alpha^{-1})E_A . \end{aligned} \tag{2.11}$$

This just cancels the contribution from $\delta\tilde{K}_C$, which suggests how accurate the on-shell approximation of II is for Ps. Curiously, if $m_1 \neq m_2$, the contribution is $(m_1-m_2)^2/(m_1+m_2)^2\alpha^2\ln(\alpha^{-1})E_A$.

We have not yet considered antiparticle poles or photon poles (I). The transverse-photon poles from the p_0 integration contribute linear terms, in the relative three momenta, to the denominators of that loop. A typical integral is then of the form [Fig. 2(b)]

$$\frac{\alpha^2}{m}\int \frac{d^3p}{|\vec{p}|^3}\frac{|\vec{p}|^2}{|\vec{p}-\vec{q}|^2}\frac{d^3q}{|\vec{q}|^2+\gamma^2}E_A ,$$

where the extra $|\vec{p}|^2$ in the numerator comes from

the transverse photon convection currents. The only order $\alpha^2 E_A$ contribution is from the relativistic region, where $p,q \sim m$, and no $\ln(\alpha^{-1})$ terms can occur. Because the annihilation kernel is nonsingular at threshold, neither the antiparticle poles nor the crossed-ladder graphs are singular enough to contribute to $\ln(\alpha^{-1})$. The renormalized vertices and propagators that occur in the αE_A calculations have logarithmic contributions which are of the size $\alpha|\vec{p}|^2 \ln(|\vec{p}|^2)$. These can only contribute to $\ln(\alpha^{-1})$ [and $\ln^2(\alpha^{-1})$] terms in order $\alpha^3 E_A$.

We do not include more than three photons in Fig. 2 because the order of the contribution from the logarithmic region ($k \gg \alpha m$) for any graph is simply its naive order, up to factors of ln α (i.e., α^{3+n}, where n is the number of photons). Some graphs having three loops or more contribute in the nonrelativistic region ($k \sim \alpha m$), but these were all explicitly calculated in II and found not to have logarithms.

The logarithmic contributions of the kernels in Fig. 2 are summarized in the first column of Table IV. There is a net contribution of $\frac{1}{6}\alpha^2 \ln(\alpha^{-1}) E_A$ to the hfs, the coefficient being fortuitously quite small. However, because the contributions δE_{TC} and δE_{AC} had been found previously,[3,4] the change in the theoretical prediction is quite large, i.e., $\alpha^2 \ln(\alpha^{-1}) E_A$. This contribution was included in the theoretical value of I (see note added in proof of I). We repeat in Table I the comparison with experiment. This new contribution, 0.023 GHz, is in fact approximately the whole contribution from $\alpha^2 \ln(\alpha^{-1})$ terms in Ps.

Some terms of the form $\alpha^2 E_F \sim 0.006$ GHz (II) and $\alpha^2 E_A \sim 0.005$ GHz (Ref. 15) have been calculated. The experimental uncertainty is only 0.0012 GHz, and clearly all terms of the above form must be calculated for a meaningful comparison with experiment to be possible. There are also certainly terms of

$$O[\alpha^2(\alpha/\pi)\ln^2(\alpha^{-1})(E_F, E_A)] \sim 0.0003 \text{ GHz}$$

(Ref. 16) which should be computed. These terms are not too difficult to find analytically.

TABLE IV. Logarithmic contributions to orthopositronium energy and decay rate coming from annihilation kernels. E_A is the lowest-order annihilation energy; Γ_0 is the lowest-order (three-photon) annihilation decay rate. The corresponding diagrams for hfs are shown in Fig. 2.

	$\alpha^2 \ln(\alpha^{-1}) E_A$	$\alpha^2 \ln(\alpha^{-1}) \Gamma_0$
T (2a)	1	1
TC (2b)	$-\frac{1}{3}$	$-\frac{1}{3}$
A (2c)	0	0
AC (2d)	$-\frac{1}{2}$	-1
D (2e)	$+\frac{1}{4}$	$+\frac{1}{4}$
DC (2f)	$-\frac{1}{4}$	$-\frac{1}{4}$
Total	$\frac{1}{6}$	$-\frac{1}{3}$

III. CALCULATION OF THE $\alpha^2 \ln(\alpha^{-1})\Gamma_0$ CONTRIBUTIONS TO POSITRONIUM DECAY RATE

The decay rate Γ of a bound state is related to its energy by[17]

$$\Gamma = -2\,\mathrm{Im}(E)\,.$$

Thus the methods of Sec. II, where we calculated the real part of the energy of o-Ps, can just as well be applied to calculating the imaginary part of the energy. This requires that at least one of the kernels have an imaginary part, i.e., be above threshold. o-Ps must decay to an odd number of photons by C invariance, so the leading contribution to the decay rate will come from the three-photon annihilation kernel. This gives the usual lowest-order decay rate Γ_0 first calculated by Ore and Powell.[7]

The calculation of the $\alpha^2 \ln(\alpha^{-1})\Gamma_0$ terms is identical to that of hfs, except that now the two annihilation kernels are different (one is to three photons). This provides an additional factor of 2 to those graphs with two annihilation kernels [2(c) and 2(d)]. The results, in terms of the lowest-order decay rate Γ_0, are recorded in Table IV. The comparison to experiment is made in Table II.

For parapositronium, the lifetime calculation is the same as for orthopositronium except that the single-photon annihilation kernels are exactly zero. The corresponding result for the logarithmic terms is

$$\Delta\Gamma = (1 - \tfrac{1}{3})\alpha^2 \ln(\alpha^{-1})\Gamma_0 = \tfrac{1}{3}\alpha^2 \ln(\alpha^{-1})\alpha^5 m\,.$$

Experimental errors are much greater than the above value, and no significant comparison with experiment is possible.

Logarithmic terms do not arise from the integration over final-state photons in the three-photon kernel [Fig. 4(a)]. We do not expect such terms to

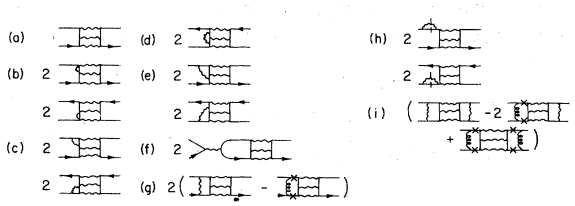

FIG. 4. Kernels contributing to order $\alpha\Gamma_0$ decay of orthopositronium. Each diagram is summed over all six intermediate photon permutations.

arise because we are far away from threshold for this diagram. In fact, here $s=(2m+\epsilon)^2$, $t=0$ while the three-photon threshold is at $s=0$, $u=4m^2$ or $t=4m^2$. Consequently, the three-photon annihilation kernel (when summed over all six photon permutations) may be expanded for small three momenta $\vec{p}$ and $\vec{q}$, about $\vec{p}=\vec{q}=0$:

$$\tilde{K}_{3\gamma}(\vec{p},\vec{q}) = \tilde{K}_{3\gamma}(0,0) + \tilde{K}^{(1)}_{3\gamma}(0,0)(\vec{p}^2+\vec{q}^2) + \tilde{K}^{(2)}_{3\gamma}(0,0)\vec{p}\cdot\vec{q} + \text{spin terms} + \cdots . \tag{3.1}$$

The coefficients $K_3^{(i)}(0,0)$ are finite. We have checked this by hand—essentially a check for the presence of anomalous thresholds. Furthermore, each term is infrared (IR) finite when convoluted with the o-Ps wave function (an IR divergence would appear as the binding energy goes to zero). A simple direct proof is simply to note that any Bloch-Nordsieck-type cancellation between radiative and virtual photons would require that the IR cancellation occurs against a two-photon final state. The matrix element for o-Ps $\to 2\gamma$ is strictly zero by charge conjugation invariance, and so for o-Ps the infrared divergences of Fig. 4(a) that are introduced when we put the electron and positron on-shell must exactly cancel among themselves. This is not explicitly true (in Feynman gauge) unless we sum over all photon permutations. The coefficients of the Taylor series (3.1) are independent of the binding. Further, the second-order terms cannot lead to an $\alpha^2\ln(\alpha^{-1})$ term because the integral of such a term convoluted with the o-Ps wave function, $\int p^2 d^3p/(p^2+\gamma^2)^2$, is not logarithmically divergent. The annihilation kernels to one, two, and three photons are all nonsingular so that the above considerations hold for each of them. Thus the calculations of Secs. II and III are identical.

There are uncalculated terms of $O(\alpha^2\Gamma_0)$ $\sim 0.0004\ \text{sec}^{-1}$ that come from many sources. These are probably small (less than $\sim 5\alpha^2\Gamma_0$). However, recall that the $(\alpha/\pi)\Gamma_0$ coefficient is rather large, ~ -10.

The results of Paper II allow us to simply read off the contributions to the coefficient of $\alpha^2\Gamma_0$ that come from multi-Coulomb exchanges ($\tilde{R}$ terms). Recalling that there is an extra factor of 2 in the diagram with two annihilations, we find from Table I of II:

$$\begin{aligned}(\Delta\Gamma)_R &= 4\alpha^2\Gamma_0(\delta\Gamma_{AT}+\delta\Gamma_{AC}+2\delta\Gamma_{AA}) \\ &= 4\alpha^2\Gamma_0\left(\tfrac{7}{16}-\tfrac{1}{24}\pi^2+\tfrac{1}{32}-\tfrac{1}{96}\pi^2-2\times\tfrac{3}{16}\right) \\ &= \alpha^2\Gamma_0\left(\tfrac{3}{8}-\tfrac{5}{24}\pi^2\right) = -1.68\alpha^2\Gamma_0 .\end{aligned} \tag{3.2}$$

The factor of 4 is the ratio of $\alpha^4 m_e$ to the annihilation energy E_A [Eq. (2.1)]. There are many other nonrelativistic contributions. Potentially the largest come from the expansion of the lowest-order diagram, Fig. 4(a), and these are also the easiest to calculate, should the difference between theory and experiment persist.

IV. CONCLUSIONS

We have now calculated all of the order $\alpha^2\ln(\alpha^{-1})$ contributions to hfs in Ps. We believe that II presents a reasonable organization of the calculation of the Ps ground-state splitting and that the calculations of this paper support that contention. There remain many $\alpha^6 m_e$ contributions to be calculated (all one-, two-, and three-photon kernels), though a start has been made.[2,15] The evaluation of the entire $O(\alpha^6)$ ground-state splitting in positronium (and muonium) is among the most important remaining high-order QED calculations.

Our original motivation for this calculation was to strengthen the theoretical prediction for the decay rate of o-Ps, and to possibly explain the significant difference between the $O(\alpha\Gamma_0)$ result and the measured decay rate. Since we completed the $\alpha^2\ln(\alpha^{-1})\Gamma_0$ calculation, the experimental rates have decreased significantly (Table II). We believe the present measured decay rate is in adequate agreement with theory, and that the theory of the calculation of bound-state decay rates is successfully tested to this order [0.25%, $O(\alpha^2\ln(\alpha^{-1}))$].

ACKNOWLEDGMENTS

We gratefully acknowledge useful conversations with Jonathan Sapirstein and Stanley J. Brodsky. This work was supported by the Department of Energy, and by the NSF.

APPENDIX: REVIEW OF THE CALCULATION OF O-Ps LIFETIME TO $O(\alpha\Gamma_0)$

The kernels which can contribute to the decay of o-Ps to order $\alpha\Gamma_0$ are listed in Figs. 4(a)–(h).[8] The virtual photons are in the Coulomb gauge.[18] These are all the kernels necessary to $O(\alpha\Gamma_0)$ because of the infrared-finite behavior of the transverse photon and the closeness of the Coulomb photon to the unperturbed kernel [see $i\delta\tilde{K}_C$ of Eq. (2.6a)]. The power counting (and the diagrams necessary) is much more complex in Feynman gauge.

We add in terms such as Fig. 4(i), which in Coulomb gauge is explicitly of order $\alpha^2\Gamma_0$. The result is that the imaginary part of the diagram of Fig. 4 is, to $O(\alpha\Gamma_0)$, equal to the square of the matrix element $\mathfrak{M}$ of Fig. 5. Note that subtractions in Figs. 4(g) and 4(i) exactly cancel the contribution to $\mathfrak{M}$ from 4(a), when the bound-state equation is used to remove iterations of the unperturbed kernel $\tilde{K}_0$. The lowest-order rate now comes

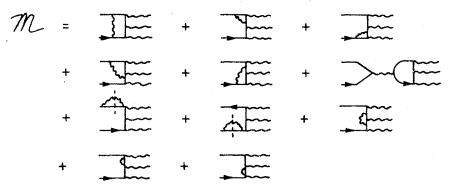

FIG. 5. Matrix element which, when squared and integrated over final photon states, gives $\Gamma_0+O(\alpha\Gamma_0)$ for positronium. A ground-state (o-Ps) wave function is convoluted on the left.

from the linear threshold singularity in the first term of $\mathfrak{M}$. In both Figs. 4 and 5 there is assumed to be an integral over the unperturbed o-Ps wave function and all external electron and positron legs are projected onto on-shell spinors (II).

It is much more convenient to calculate on-shell amplitudes. The electron and positron are only slightly off-shell, and it is easy to see that there are only corrections of $O(\alpha^2\mathfrak{M})$ coming from putting all but the first term of $\mathfrak{M}$ on-shell. This is true because each diagram *separately* is IR finite in Coulomb gauge up to corrections of order

$$\langle (k^2/m^2)\ln\lambda\rangle \alpha\Gamma_0 \sim \alpha^3\ln(\alpha)\Gamma_0$$

in the rate. The wave function has on-shell spinors, and so putting the external legs on-shell makes no difference to them. The first term in $\mathfrak{M}$ can also be placed on-shell (retaining only the real part), even though it has a linear Coulomb singularity at threshold. To see this, we examine the difference between this diagram on- and off-shell when convoluted with the wave function. Neglecting terms which are IR finite (these cancel to order α), we need only consider the Coulomb part of the exchange photon, and that only in the nonrelativistic region. Using Eq. (2.2), the leading low-momentum contribution to the first (singular) term of $\mathfrak{M}$ is

$$\mathfrak{M}_{\rm div} \approx \int \frac{d^3p}{(2\pi)^3}\,\phi(\vec{p})\,\frac{i\tilde{K}_C(\vec{p},\vec{q})}{P_0-E_1(\vec{q})-E_2(\vec{q})}\,\frac{d^3q}{(2\pi)^3} \times \bar{v}(-\vec{q})\mathfrak{M}_{3\gamma}(0)u(\vec{q}). \tag{A1}$$

The effect of putting the external legs on-shell is simply to let $P_0\to E_1(\vec{p})+E_2(\vec{p})$. The difference between the two cases is

$$\begin{aligned}\mathfrak{M}_{\rm div}-{\rm Re}(\mathfrak{M}_{\rm o.s.}) &= {\rm Re}\int\frac{d^3p}{(2\pi)^3}\,\phi(\vec{p})i\tilde{K}_C(\vec{p},\vec{q})\left(\frac{1}{P_0-E_1(\vec{q})-E_2(\vec{q})}-\frac{1}{E_1(\vec{p})+E_2(\vec{p})-E_1(\vec{q})-E_2(\vec{q})}\right)\frac{d^3q}{(2\pi)^3}\,\tilde{\mathfrak{M}}_{3\gamma}(0)\\ &\simeq\left(\frac{\gamma^3}{\pi}\right)^{1/2}{\rm Re}\int\frac{\gamma}{\pi^2}\,\frac{d^3p}{(\vec{p}^2+\gamma^2)^2}\,\frac{-e^2}{|\vec{p}-\vec{q}|^2}\,\frac{(-m)(\vec{p}^2+\gamma^2)}{(\vec{q}^2+\gamma^2)(\vec{p}^2-\vec{q}^2)}\,\frac{d^3q}{(2\pi)^3}\,\tilde{\mathfrak{M}}_{3\gamma}(0)\\ &=0+0(\alpha^2\ln(\alpha^{-1})\Gamma_0).\end{aligned} \tag{A2}$$

The second line follows by making the leading nonrelativistic approximation for all terms, including the wave function. The last follows from the antisymmetry of the resulting integral in p and q. Had this difference not been zero, it might still have been useful to make these transformations. We could then have evaluated the above integral to $O(\alpha\mathfrak{M}_{3\gamma})$ and still been able to do the rest of the problem as we do in the following.

We have reduced the necessary matrix element to an on-shell $e^+e^-\to 3\gamma$ scattering amplitude. This may be evaluated, by the usual arguments,[13] in any gauge, and it is here that we choose to work in Feynman gauge. It is only here that the external propagator corrections ($4h$) are removed from the problem (by renormalization). It is clear from the Coulomb-gauge derivation that there are no real IR divergences left in this problem. A direct proof follows that of Sec. IV for the lowest-order decay kernel, i.e., virtual corrections to three-photon decay cannot cancel against four-photon decay, by C invariance. The rest of the calculation is then as described in Ref. 8.

We have improved the numerical uncertainty on the most difficult of the $O(\alpha\Gamma_0)$ contributions, $\Gamma^s_{g'}$, of Ref. 8. Symmetrizing the integral in the physical three-momentum ($\vec{k}\to-\vec{k}$) allowed us to obtain an accurate value without any extrapolation. The improved value is

$$\Gamma^s_{g'}=(-5.818\pm0.008)(\alpha/\pi)\Gamma_0.$$

It is included in the theoretical value quoted in Table II. The value in Table II was previously quoted in Ref. 11. The logarithmic contributions to the decay rate calculated in Sec. III allow us to make a more precise comparison to experiment. The comparison to the most recent precision o-Ps decay measurements is made in Table II.

*Present address.

[1]G. P. Lepage, Phys. Rev. A 16, 863 (1977); to be referred to as Paper I. These results have been verified by G. T. Bodwin and D. R. Yennie, Phys. Rep. 43C, 267 (1978).

[2]W. E. Caswell and G. P. Lepage, Phys. Rev. A 18, 810 (1978); to be referred to as Paper II. An almost identical formalism has been independently derived

by R. Barbieri and E. Remiddi, Nucl. Phys. B 141, 413 (1978), for positronium.
[3]D. A. Owen, Phys. Rev. Lett. 30, 887 (1973); R. Barbieri, P. Christillin, and E. Remiddi, Phys. Lett. B 43, 411 (1973).
[4]R. Barbieri and E. Remiddi, Phys. Lett. B 65, 258 (1976).
[5]P. O. Egan, W. E. Frieze, V. W. Hughes, and M. H. Yam, Phys. Lett. A 54, 412 (1975).
[6]A. P. Mills, Jr. and G. H. Bearman, Phys. Rev. Lett. 34, 246 (1975).
[7]A. Ore and J. L. Powell, Phys. Rev. 75, 1696 (1949).
[8]W. E. Caswell, G. P. Lepage, and J. R. Sapirstein, Phys. Rev. Lett. 38, 488 (1977).
[9]D. W. Gidley, K. A. Marko, and A. Rich, Phys. Rev. Lett. 36, 395 (1976); D. W. Gidley, P. W. Zitzewitz, K. A. Marko, and A. Rich, Phys. Rev. Lett. 37, 729 (1976).
[10]T. C. Griffith and G. R. Heyland, Nature (London) 269, 109 (1977).
[11]D. W. Gidley, A. Rich, P. W. Zitzewitz, and D. A. K. Paul, Phys. Rev. Lett. 40, 737 (1978).
[12]D. W. Gidley and P. W. Zitzewitz, Phys. Lett. A (to be published).
[13]We use the notation of J. D. Bjorken and S. D. Drell, *Relativistic Quantum Mechanics* (McGraw-Hill, New York, 1964), except that we normalize $\bar{u}u = -\bar{v}v = 2m$.
[14]For simplicity in keeping track of signs (especially to have the same trace algebra on each leg), we have chosen to use a particle-particle bound-state formalism (as opposed to a particle-antiparticle formalism). This is possible because we always, in the logarithmic momentum region, take the annihilation kernel to be momentum independent (a position-space δ function), and thus it factors out. Thus for us particle 1 has charge e, and particle 2 has charge $-e$. An antiparticle formalism would simply let $u \to \bar{v}$ for particle 2, both particles would have the same charge, and there would be a minus sign for all nonannihilation kernels (but not for annihilation kernels).
[15]R. Barbieri, P. Christillin, and E. Remiddi, Phys. Rev. A 8, 2266 (1973); V. K. Cung, A. Devoto, T. Fulton, and W. W. Repko, Phys. Lett. B 68, 474 (1977); Nuovo Cimento A 43, 634 (1978), and preprints, MSU (March, 1978) and Johns Hopkins (August, 1978).
[16]A. J. Layzer, Nuovo Cimento 33, 1538 (1964); D. E. Zwanziger, Nuovo Cimento 34, 77 (1964).
[17]M. L. Goldberger and K. M. Watson, *Collision Theory* (Wiley, New York, 1964), Chap. 8.
[18]In Coulomb gauge the wave-function renormalization constant Z_2 is a momentum-dependent spinor matrix. The dashed lines through the external propagators in Fig. 4(h) emphasize that half of the renormalized fermion propagator must be associated with the perturbation kernel and half with the binding kernel $\tilde{K}_0$. Then Ward's identity can be satisfied order by order in the coupling. The external fermions are approximately on-shell when calculating the $O(\alpha\Gamma_0)$ decay rate, so we need only renormalize the lowest-order $u(p)$ and $v(p)$ [i.e., we need only the part of Z_2 with a nontrivial spinor structure; the remainder after renormalization is $O(\alpha^2)$].